*Near Surface Geophysics, 2009,* 413-425

# Aquifer investigations in the León-Chinandega plains, Nicaragua, using electromagnetic and electrical methods

Marvin Corriols[1,3*], Mette Ryom Nielsen[2], Torleif Dahlin[3] and Niels B. Christensen[4]

[1] *Centro de Investigaciones Geocientificas, GIGEO-UNAN, Colonia Miguel Bonilla Casa #165, Managua, Nicaragua*
[2] *Rambøll, Vand & Miljø, Bredevej 2, 2830 Virum, Denmark*
[3] *Department of Engineering Geology, Lund University, Box 118, 221 00 Lund, Sweden*
[4] *Department of Earth Sciences, Aarhus University, Hoegh Guldbergs Gade 2, 8000 Aarhus C, Denmark*

Received October 2008, revision accepted June 2009

**ABSTRACT**

The Leon-Chinandega plains are located in the north-western part of Nicaragua and represent the most important groundwater reservoir of the country. The aquifer is comprised of three hydrogeological units. The top unit is an unconfined alluvial and below a more consolidated volcanic aquifer is found. These aquifers rest on an ignimbrite unit that acts as the basement of the aquifer. The plains are mainly used for agricultural purposes and most of the irrigation comes from upper aquifer wells (not deeper than 70 m) allocated within the shallow unconfined aquifer.

Transient electromagnetic soundings (TEM) and continuous vertical electrical soundings (CVES) were carried out in order to obtain information regarding the geology of the study area. Two TEM profiles extending from the Pacific coast towards the volcanic chain were carried out with an approximate separation between soundings of 250 metres. A grid of TEM soundings was also performed in an area located between the towns of Posoltega and Quezalguaque. CVES were carried out in different areas of the plains in order to obtain detailed information on the geology and distribution of the shallow aquifer. This information was later correlated with information available from wells in the area.

One of the objectives of this investigation was to test and evaluate the applicability of the TEMfast48 equipment in the study area. In the plains area the TEM method shows very good results where a general geophysical model of mostly a three-layered earth can be obtained. In the coastal areas the models are more irregular and complex. The results from the CVES generally agree with the TEM models but present more details, especially in areas of complex geology. The penetration depth for the TEM soundings reached almost 100 m at most, depending on the depth to a low resistivity layer. In some areas the depth to the basement was estimated with long-layout CVES.

In general, it was possible to obtain consistent geoelectrical models of the area and the methods complement each other well. The geoelectrical models are an excellent addition to other investigation methods as they provide an overview of the aquifer system and can serve as a basis for refining the conceptual and numerical models of the aquifer system. This information is expected to become very valuable for the exploration, management and protection of the groundwater resources in the León-Chinandega plains to ensure sustainability of the resource.

## INTRODUCTION

The León-Chinandega plains are situated parallel to the coast line in the north-western part of Nicaragua. The study area extends from the coastal area towards the Nicaraguan volcanic chain (see Fig. 1). The León-Chinandega plains can be divided into three major physiographic units; the active volcanic chain (with altitudes above 300 m.a.s.l.), the volcanic foothills (from 300–100 m.a.s.l.) and the plains with altitudes ranging from 100–0 m.a.s.l. For the present study a smaller area in the central part of the plains between the towns of Posoltega and Quezalguaque was selected for detailed geophysical investigations.

In previous years, the plains were used for extensive cotton farming and poorly managed use of pesticides caused the groundwater quality to deteriorate. Recent studies show that

* marvin@cigeo.edu.ni

there are areas within the plains with high levels of pesticide pollution (Briemberg 1994; Lopez *et al.* 2000; Dahlberg and Odebjer 2002; Delgado 2003; Moncrieff *et al.* 2008). Most of the contamination is found in shallow excavated wells in the top portion of the upper alluvial aquifer. The public drinking water supply systems for the major cities in the plains are supplied from deeper wells allocated mostly in the lower parts of the upper alluvial aquifer and at the top portion of the deeper volcanic aquifer. A study carried out by Briemberg (1994) showed that some of these public water supply wells were already polluted.

People living in small communities within the plains have their own shallow excavated wells and therefore are directly exposed to pesticides. One of the biggest environmental concerns in the area is the migration of the contaminants found in the shallow parts of the aquifer to the deeper parts, leading to a more serious environmental problem in the area.

## GEOLOGY

The study area is dominated by four geomorphologic units, the León-Chinandega plains, the volcanic foothills, the Nicaraguan volcanic chain and the Tamarindo Plateaus. The first is an extended volcanic plain between 0–100 m.a.s.l.; it starts at the slopes of the volcanic chain (volcanic foothills) and ends at the Pacific coast. The topographic gradient is very low, around 0.6%. In areas of discharge of rivers and estuaries, the terrain becomes swampy, a product of the shallow water table and tidal processes. The volcanic foothills are located between 100–300 m.a.s.l. with gentle slopes around 3%. The Nicaraguan volcanic chain is located at the north-eastern boundary of the study area and is a natural watershed divide. The volcanic structures can vary from partly degraded units due to erosion and tectonic events, to well formed volcanic cones from recent volcanic activity. The lava composition ranges between andesites, dacites, normal basalts and olivine basalts. The volcanoes are associated with an increasingly steep topography with altitude, the slopes range from 36–71%.

The Tamarindo Plateaus are hills comprised of Tertiary volcanic rocks reaching elevations up to 300 m.a.s.l. The major outcrops are located west of the city of Leon with isolated occurrences along the coast.

The León-Chinandega plains are comprised of three geological units: the alluvial and pyroclastic Quaternary deposits, which cover most of the surface of the area, the Las Sierras Formation underlying the quaternary deposits and the Tamarindo Formation, which is the basement. The upper two units are considered the main aquifer units.

The Tamarindo Formation has been studied by several authors, such as Wilson (1942), Kuang (1971) and McBirney and Williams (1965). This formation has been defined as a sequence of volcanic ignimbrites and andesitic lavas by Wilson (1942), who named these sequences as the Tamarindo Formation based on the existence of an extensive outcrop in the Tamarindo River.

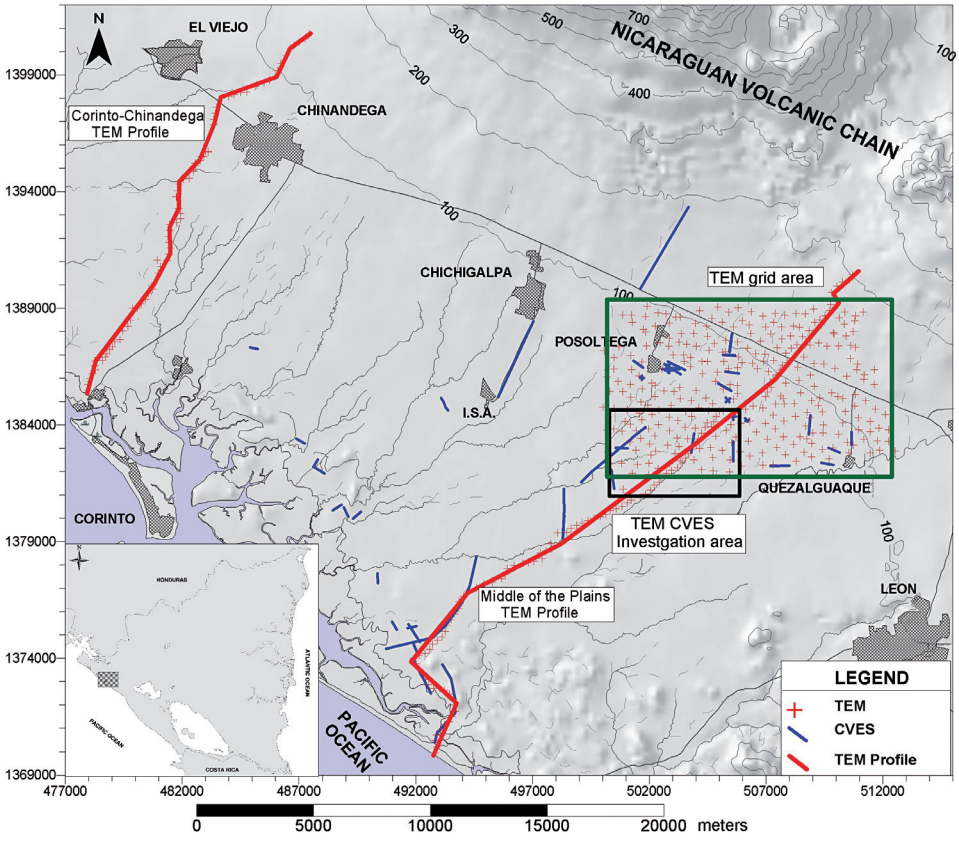


FIGURE 1
Location map of the study area with CVES and TEM sounding locations.

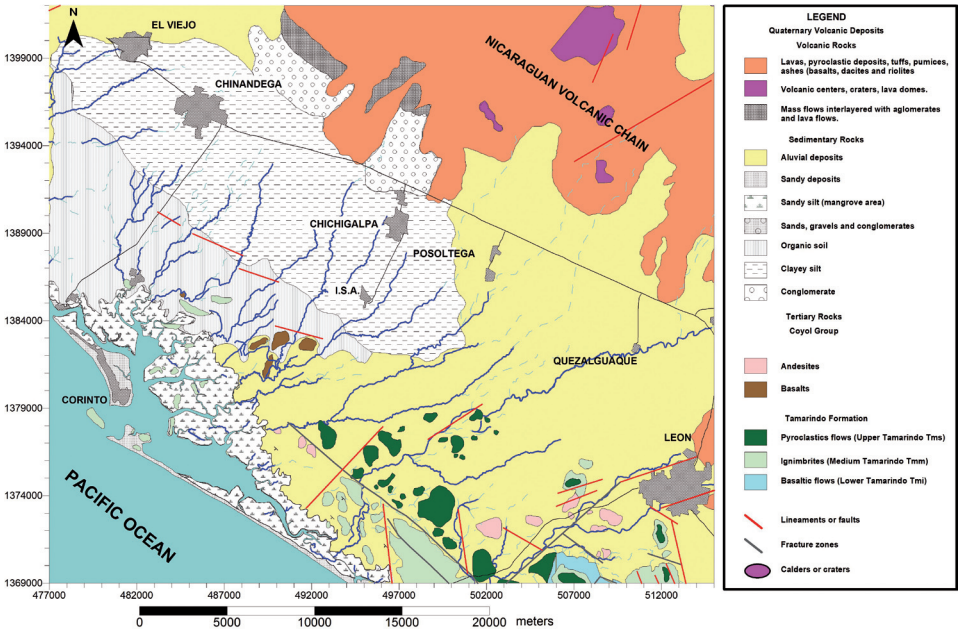


FIGURE 2
Geological map of the study area in the León-Chinandega plains (Modified from CIGEO 1999).

The Tamarindo Formation extends in a fringe oriented NW-SE and parallel to the coastline and has been subdivided into three members based on the lithological composition of the different volcanic sequences. The Miocene-Pliocene Tamarindo Formation has an age of 14.8 ±0.5 million years (Elming *et al.* 2001). The Lower Tamarindo Formation is approximately 200 m thick and it is the only lava flow of andesitic-basaltic composition that is definitively older than the ignimbrites that belong to the Medium Tamarindo Formation. The ignimbrites are generally homogeneous and of rhyolitic composition. The colour of these rocks is a rosy shade and in outcrop they exhibit spheroidal weathering, giving rise to a sandy detritus produced by the disaggregation of the granular components. The thickness of the unit is approximately 175 m. The Upper Tamarindo Formation is made up by several pyroclastic flows, with an approximate total thickness of 100 m. The deposits are characterized by very high concentrations of quartz and plagioclase crystals. Occasionally the enrichment of quartz and plagioclases in the tuffs makes them resemble an acid intrusive rock.

The Las Sierras Group consists mainly of a diverse variety of pyroclastic materials such as tuffs (lithic and agglomeratic) and pumice (Kuang 1971). The tuffs are always intercalated with ashes, breccias and volcanic scoria; they have a regular compaction and are partially weathered. At the bottom of the Las Sierras Group, a clay layer formed by weathering processes overlies the ignimbrites of the Tamarindo Formation.

The Pleistocene-Pliocene age for the Las Sierras Formation was inferred from their lithological characteristics (Zoppis-Bracci and Del Guidicce 1958). The thickness of the formation is around 220 m (United Nations 1974).

The pyroclastics and alluvial deposits discordantly overlie Las Sierras tuffs and, in some coastal regions, the Tamarindo Formation. Silts, fine to coarse sands, ashes, lapilli, pumice and gravels constitute the deposits. During the sedimentation process, the coarser sediments have been deposited close to the volcanic chain and the fine ones close to the coast. The deposits are Upper-Pleistocene to recent in age (United Nations 1974).

The sedimentary deposits, which are products of the disintegration, transportation and deposition of volcanic materials, occupy large areas on the Leon-Chinandega plains. The Quaternary sediments range from sandy to silty-sandy materials and packages of stratified conglomerates, sands and gravels. The thickness of the deposits ranges from a few metres to 120 m.

The Quaternary volcanic deposits include derivative products of the volcanic chain. Those products have been deposited from the Pleistocene to the recent. The deposits consist of sequences of interstratified basaltic, andesitics and rhyolitic lavas and stratified pyroclastic materials that include pumice and tuffs with lapilli structures. The chemical composition of the magma in this region is basaltic with its subordinate dacitic and rhyolitic variants.

## HYDROGEOLOGY OF THE AREA

Two different flow systems are expected in the León-Chinandega aquifer. The first one is a shallow flow system, locally recharged in the central and low parts of the plain, discharging into springs, rivers and pumping wells. The second system is a deep regional flow system, recharged at the volcanic chain and discharged in the central and lower parts of the plain (Calderon 2003; Calderón and Bentley 2007).

According to INETER (2000) four recharge zones have been defined according to their soil characteristics. The recharge values are expressed as percentages related to the annual average precipitation. The zone of the volcanic slopes (located above 150 m.a.s.l.) presents the highest infiltration rates (38–46%) and

represents the principal recharge area of the aquifer. It consists mainly of sandy loams and coarser materials that facilitate the infiltration process. The estimated annual average precipitation is between 593–881 mm.

In the central part of the plains (located between 20–150 m.a.s.l.) the recharge is around 20–35 % and the soils are mainly composed of loams and sandy loams. The cultivated soils play an important role in the infiltration process in the plains with an infiltration capacity four times greater than the non-cultivated soils (United Nations 1974). The estimated annual average precipitation ranges between 316–678 mm.

The third recharge zone is located south-west of the plains, (between 10–20 m.a.s.l.) and is characterized by loams and clayey loams. The recharge ranges from 0–10%, with the lower values towards the coast and the annual average precipitation is estimated to be between 0–146 mm. This zone represents the discharge area of the aquifer.

The final recharge area (0–10 m.a.s.l.), is located between the mangrove area and the Pacific Ocean coast and represents the rejected and lateral recharge zone of the aquifer. The rejected recharge occurs in the lowlands (near the coast) and is caused by the oversaturation of the clayey soils; the lateral recharge occurs in areas where the Tamarindo Formation outcrops and in those areas the rainwater runs off towards the plains and either infiltrates into the aquifer or is evaporated. The amount of water that infiltrates is not significant to the total recharge of the aquifer (INETER 2000).

## PREVIOUS GEOPHYSICAL STUDIES

No recent geophysical studies have been carried out in the study area, the first and only one being carried out by the United Nations during the early 1970s. After 1999, a cooperation project between Lund University and Autonomous National University of Nicaragua (UNAN-Managua) carried out geophysical investigations to obtain information regarding the geometry of the aquifer in the area. This information was later correlated with the available geological information and geo-electrical cross-sections and a basement map were constructed (Corriols 2003; Corriols and Dahlin 2008). Continuous vertical electrical soundings (CVES) and transient electromagnetic soundings (TEM) (in cooperation with Aarhus University) were used to map the shallow parts of the aquifer (Corriols 2003; Ryom 2004; Cáceres 2005; Corriols and Dahlin 2008).

## METHODOLOGY

Among all geophysical techniques, electrical and electromagnetic methods are undoubtedly the leading ones in exploration and management of groundwater (Goldman and Kafri 2006). Both techniques are mostly used to obtain information regarding the geometric features of the aquifer, such as, fresh-saline groundwater interface, distinction between clay and sand, thickness and depth of alluvial fill and gravel lenses, depth to the water table, etc.

### TEM

The TEM method is an inductive time-domain electromagnetic method that maps the electrical resistivity of the ground. The TEM method has proven to be useful for mapping geological structures of hydrogeological relevance (Christiansen and Christensen 2003; Auken *et al.* 2003). The method is especially optimal for mapping the depth to conductive formations, e.g., clay, often representing the bottom of aquifers.

#### *TEM data acquisition*

For the TEM investigations in the León-Chinandega plains the compact and lightweight TEMfast 48 system was applied. Prior to the field campaign in Nicaragua, the TEMfast 48 system was tested at the Lyngby TEM-test site outside Aarhus in Denmark (Hydrogeophysics Group 2002) in order to obtain optimal configuration information and necessary system-details. The tests showed that the 25 m × 25 m coincident loop configuration and a maximum recoding time of 2 ms were the most optimal setting and configuration for the system. With this configuration and a transmitted current of 1 A, the tests gave a turn-off time of 3.0 $\mu$s and a repetition frequency of 100 Hz. Calibration revealed the necessity of a time shift of 0.5 $\mu$s and an amplitude factor of 1.14. The calibration also revealed a system bandwidth limitation of 250 KHz, which must be included in the inversion (Effersø *et al.* 1999). A more detailed description of the tests and conclusions is found in the Appendix.

A total of 472 TEM soundings were collected during the field work in February–April 2003 in the León-Chinandega area. All soundings were performed with the TEMfast 48 equipment with a 25 m × 25 m coincident loop configuration. As illustrated in Fig. 1, part of the TEM soundings were placed along two profiles going from the Pacific coast towards the volcanic chain with a sounding spacing of approximately 250 m. The orientation of the profiles is southwest-northeast parallel to the main drainage direction. The remaining TEM soundings were placed in a grid between the villages of Posoltega and Quezalquaque, with a sounding spacing of approximately 500 m.

Two measurements were performed at each location, one transmitting 1 A and one transmitting the maximum possible current, which was approximately 2.2 A with the loop cable used. Measurements with 1 A have undisturbed data points at early times and should reveal information about top layers whereas measurements with a higher current should reveal information about deeper layers.

Noise measurements were performed three times a day. Generally, the noise level was low (below 5 nV at 1 ms) and interferes with the sounding only at late times, later than 1 ms. There was no obvious difference in the noise levels during the day or in different areas. As expected the noise exhibit a $t^{-1}$ dependence at early times and at later times a $t^{-1/2}$ dependence (Effersø *et al.* 1999).

At a reference location in the area, test soundings were performed once or twice a week in order to check for errors or drift

in the equipment. The reference location is located adjacent to the MI-2 borehole. All soundings at the reference location correlate and the equipment was functioning perfectly during the whole field campaign.

*Modelling, inversion and analyses*

Forward modelling of 1D responses of the TEMfast 48 system were carried out by recursively computing the kernel function in the Laplace/wavenumber domain followed by an inverse Laplace transform using the Gaver-Stehfest algorithm and transforming to the space domain using the Fast Hankel Transform filters (Christensen 1990). The forward modelling takes repetition, waveform and band limitation of the system (Effersø *et al.* 1999) into account. Derivatives with respect to the model parameters were calculated using the same numerical procedure as for the forward responses on 'analytic' kernel functions obtained by differentiating the recursion formulas for the response to ensure speed and accuracy.

The inversion approach of the TEMfast 48 data from the León-Chinandega plains is a well-established iterative damped least-squares method using 1D models consisting of horizontal, homogeneous and isotropic layers (Menke 1989). 1D inversion is carried out with both few-layer and multi-layer models. In the few-layer inversion, the layer resistivities and the thicknesses are free to vary and no constraints are applied to combinations of model parameters. Generally, the few-layer inversion aims at minimizing the data misfit using a specific, small amount of layers. In the multi-layer inversion, the layer boundaries are fixed and only the layer resistivities are free parameters. The inversion is regularized through vertical constraints ensuring identity between neighbouring layer resistivities within a given relative uncertainty.

**DC resistivity imaging – CVES**

The resistivity method measures variations in the electrical resistivity of the ground by applying small electrical currents across arrays of electrodes inserted in the ground. During resistivity surveys, current is injected into the earth through a pair of current electrodes and the potential difference is measured between one or several pair(s) of potential electrodes. The current and potential electrodes are generally arranged in a linear array. Basically there are two major ways in which electrical charges can be transported through rocks, either by electronic conductivity or by electrolytic conductivity, where the latter is most important in common geologic materials.

The resistivity readings are processed and inverted to produce sections or volumes of the resistivity distribution of the subsurface. Results are correlated with real ground interfaces such as soil and rock layering or soil-bedrock interfaces to provide information on subsurface structure.

*Data acquisition*

The CVES resistivity data were collected using the ABEM Lund Imaging System with an array of 81 electrodes. The Lund Imaging system is a computer-controlled multi-electrode data acquisition system used for two-dimensional (2D) and three-dimensional (3D) high resolution surveys, consisting of a resistivity-meter, a relay switching unit, four multi-electrode cables and stainless steel electrodes and optionally an external computer may be used in addition for a better overview of the data acquisition process. The multi-electrode cables have 21 take-outs with 5 metre spacing. The last takeout of each cable is overlapped with the first takeout of the next cable, giving a total of 81 active electrodes. When deeper penetration was needed, the spacing between electrodes was increased to 10 metres using four extension cables and four extra electrode cables. Extension of the survey can be achieved by a technique called roll-along, in which part of the original layout is shifted in the desired direction. Usually this is a quarter of the total length of the layout and new measurements are added to the survey (Dahlin 2001).

*Data processing/inversion*

The data collected during the fieldwork campaigns were processed with the inversion program RES2DINV (Loke 2001). The program is based on numerical modelling techniques using finite difference or finite element methods (Oldenburg and Li 1994; Tsourlos 1995; Loke *et al.* 2003). The method aims at reducing the differences between the resistivities measured and the calculated response of the estimated model carrying out a number of iteration steps, until satisfactory agreement between model response and field data is reached or no further improvement is possible (Dahlin 2001). The result is a two-dimensional earth profile built from mathematically modelled resistivities. In the inversion process the subsurface is divided into a number of rectangular blocks with fixed dimensions.

**RESULTS AND INTERPRETATION**

**TEM profiles**

One-dimensional (1D) inversion results with both few-layer and multi-layer models are presented for the two TEM profiles in Figs 3 and 4. Below the few-layer models the parameter analysis is presented in cells, where each cell represents a parameter. The colour of the cell indicates how well the parameter is determined. Red illustrates a well determined parameter and blue illustrates a poorly determined parameter. Below the multi-layer model section, a section representing the relative uncertainty of the resistivity parameter is found. Uncertainties of model parameters in multi-layer models are mainly determined by the vertical constraints. Instead of showing parameter uncertainties a relative uncertainty of the resistivity parameter of each layer is calculated, which describes to what degree the information from data has contributed to the resulting resistivity as opposed to the contribution from the vertical constraints. This relative uncertainty section hence shows the depth intervals where data has contributed to the resolution of the resulting resistivity (red) and where resistivities are mainly controlled by the vertical constraints (blue).

For all models, the total residual is presented. Values close to zero indicate that the model has fit the data well within the uncer-

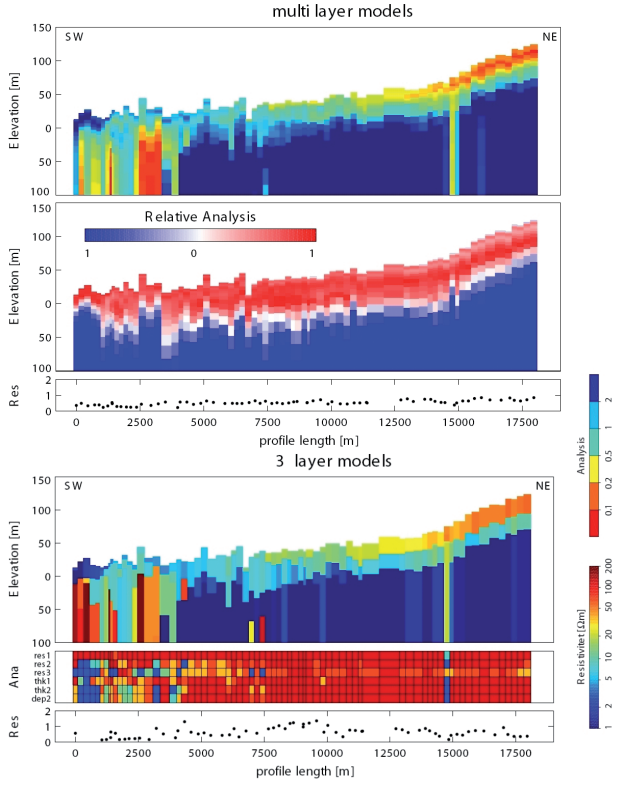


FIGURE 3
Corinto-Chinandega TEM profile. From top to bottom: multi-layer model section, a section of the relative uncertainty of the resistivity parameter of the multi-layer model, total residual of how the models have fitted the data, few-layer model section, parameter analysis of few-layer models and total residual of how the models have fitted the data.

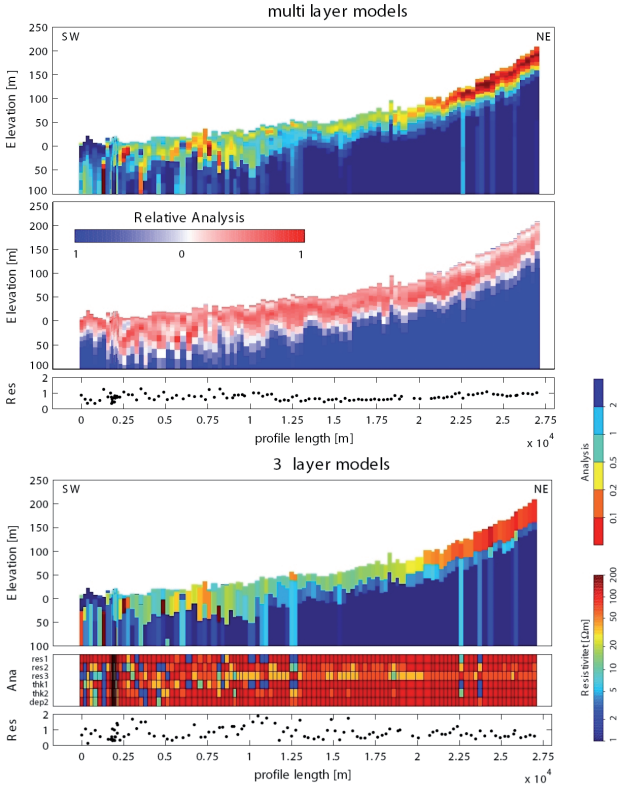


FIGURE 4
Middle of the plains TEM profile. From top to bottom: multi-layer model section, a section of the relative uncertainty of the resistivity parameter of the multi-layer model, total residual of how the models have fitted the data, few-layer model section, parameter analysis of few-layer models and total residual of how the models have fitted the data.

tainties of the data. A value of 1 indicates that the model has fitted the data with an uncertainty that equals the average uncertainty of data.

*Corinto-Chinandega profile*

Figure 3 presents the 1D inversion results of the TEM soundings in the profile from Corinto at the Pacific coast past the village of Chinandega towards the volcanic chain.

In general, both the multi-layer models and the few-layer models show regular layered models with low resistivities at depths greater than 30 m and higher resistivities in the shallower parts. In the high elevation part of the profile, i.e., the north-eastern part, resistivities between 50–100 Ωm are found in the top layer. Below this is a layer of approximately 10 Ωm and finally, below 30 m depths, is a layer with a resistivity less than 2 Ωm. In the central part of the profile the highly resistive top layer is not present. In the south-western part of the profile, close to the coast, the models are more complex and no lateral correlation between the layers can be found. The regular layered models without major variations in the majority of the section indicate the large-scale geological composition of the area. Minor local variations may be present and not resolved because of the TEM data density and because of the resolution ability of the method. The complex composition of the models in the coastal area indicates more heterogeneity in this area. The 1D inverted models in this area are potentially affected by 2D and 3D effects because of the heterogeneity. Hence the focus of the results in this area is the overall heterogeneity in the area rather than the geological understanding of each model.

The sediments in the area are derived from weathered volcanic material giving rise to a primary unconfined aquifer described in the hydrogeological framework section. Generally the high resistivities in the high elevations can be interpreted as the unsaturated zone consisting of younger rock debris that are not as weathered as the sediments below. The primary aquifer can be correlated with the second layer at high elevations and towards lower altitudes the aquifer gradually represents the first layer of the models. As also described in the hydrogeological framework section a secondary aquifer below the primary aquifer contains more clay, which corresponds to the deep good conductor. The complexity of the models in the coastal region represents ignimbrites of the Tamarindo Formation that are observed to outcrop in this region.

For most of the models, the relative analysis of the multi-layer inversion shows values close to 1 until approximately 50 m depth. This indicates that until a depth of 50 m the data has contributed to the obtained resistivity. The white colour indicates the limit between depths where data contribute to the resulting resistivity value and depths where data do not contribute much. Hence, the white zone represents a measure of penetration depth.

The total residual for the majority of the multi-layer models is below 1, which indicates that the models have fitted data within the uncertainties. As expected the residual for the few-layer models is a bit higher. Almost all parameter uncertainties for the few-layer models are below 0.2, a fairly small uncertainty. However, this is not the case in the coastal regions where only the resistivities of the first layer have a small uncertainty.

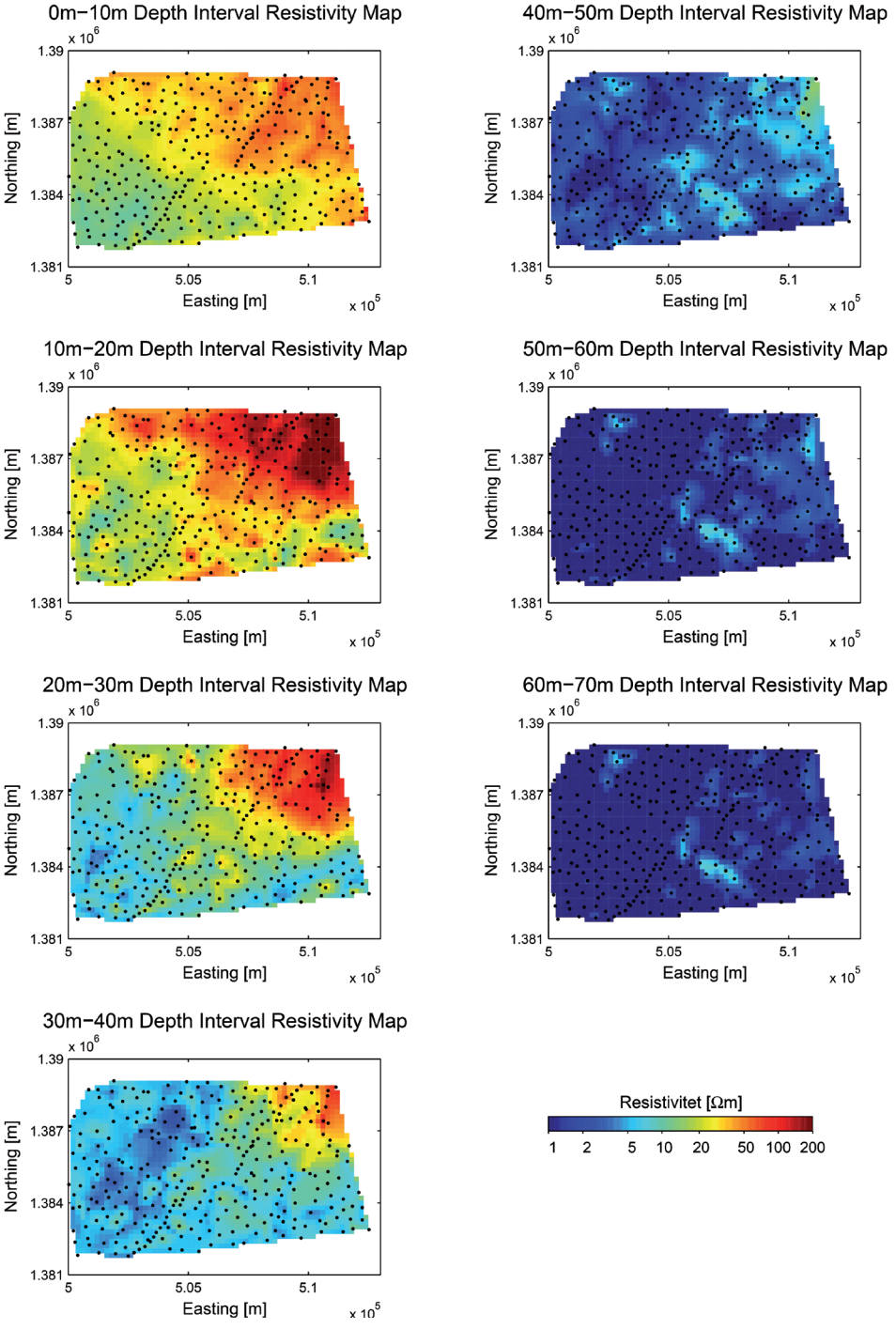


FIGURE 5
Depth interval resistivity maps based on the multi-layer model interpretations of the TEM soundings in the Posoltega-Quezalguaque area.

*Middle of the plains profile*

Figure 4 presents the 1D inversion results of the TEM soundings in the profile of the Pacific coast past the plains between the villages of Posoltega and Quezalguaque towards the volcanic chain.

The overall picture is similar to the previous profile. There is a regular layered geometry in the north-eastern part of the profile with high resistivities in the top layer and low resistivities in the deepest layer. More complex models are found closer to the coast. The penetration depths, observed in the relative analysis of the multi-layer models, are on average around 60 m, corresponding to the depth of the low-resistivity layer. As expected, the residuals for the multi-layer models are generally lower than for the few-layer models.

For the few-layer models the depth to the low-resistivity deep layer has very little uncertainty for almost all soundings. The resistivity and thickness of first and second layers have higher uncertainties. This is the case if the layer is highly resistive or very thin. In a few cases the resistivity of the third layer is uncertain. This is due to an assignment of a large total standard deviation to the last data points of these soundings. The increased standard deviation gives lower residuals since the model can more easily fit the data. However, the increased standard deviation results in higher uncertainty for the model parameter. In a few soundings the total residual is quite high and the model has not fitted the data. However, in most of these cases, these models do not vary considerably from the neighbouring models.

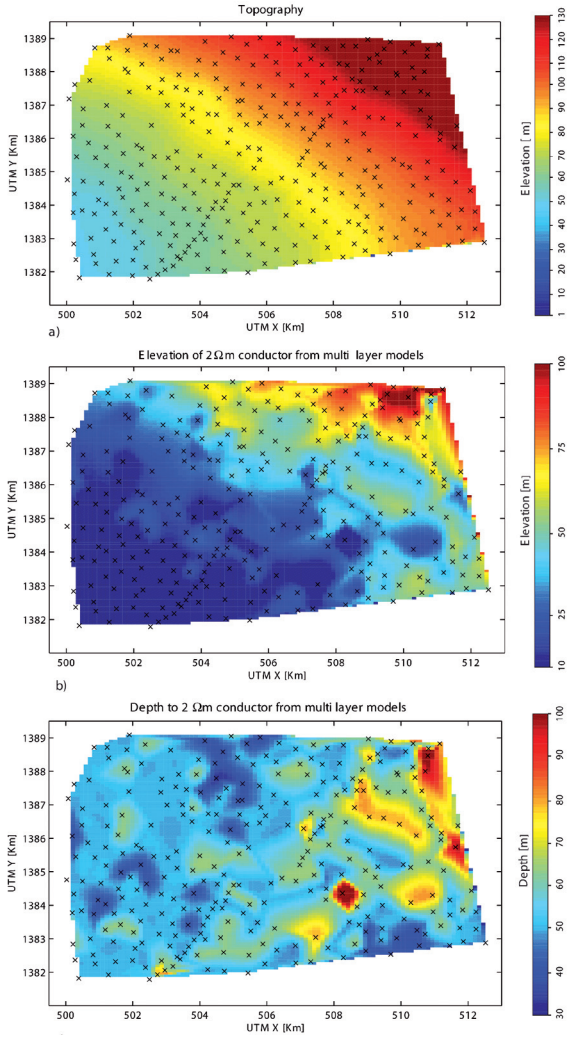


FIGURE 6

Contoured maps of, from top to bottom: topography, depth and elevation to the good conductor (deep model layer with a resistivity of 2 Ωm or less) from the multi-layer model interpretations of the TEM soundings.

**Posoltega-Quezalguaque grid**

The locations of the TEM soundings in the Posoltega-Quezalguaque grid are illustrated in Fig. 1. The data from these soundings have also been interpreted using both multi-layer and few-layer models. Only the results of the multi-layer models are presented as contoured maps of mean resistivity in depth intervals and contoured maps of depth to and elevation of the deep good conductor.

*Mean resistivity maps*

In Fig. 5, the mean resistivity maps based on the multi-layer models are presented. The first interval from 0–10 m depth shows resistivities from 30–100 Ωm in the north-eastern corner, corresponding to unsaturated young volcanic sediments and intermediate resistivities of approximately 10 Ωm, indicating the primary aquifer in the south-western corner. The resistivities in the north-eastern corner are higher in the depth interval from 10–20 m.

In the following depth intervals, the extent of this highly resistive area is reduced and disappears totally at around 50 m depth. The resistivities of the remaining area decrease gradually and in the depth interval from 60–70 m almost the entire area consists of a resistivity close to 1 Ωm, also denoted as ‘the deep good conductor’ described in the following section.

*Depth to the good conductor*

In the mean resistivity maps, values as low as 1 Ωm were found from approximately 40 m depth. In Fig. 6, a contoured map of the topography is compared to contoured maps of the elevation and depth of the good conductor. The good conductor in this case is chosen to be resistivities of 2 Ωm and less and depths are based on the multi-layer model interpretations.

The topography of the area increases gradually towards the volcanic chain to the north-east. The elevation of the surface of the conducting layers more or less follows the topography with a few anomalies. The depth to the conductor is a subtraction of the elevation of the conductor from the topography. The depth of the conducting layer reveals locations where the conductor surface does not follow the surface topography. The depth to the conductor is between 40–60 m in most of the area. In certain locations, the depth is 75 m and in three locations the depth reaches close

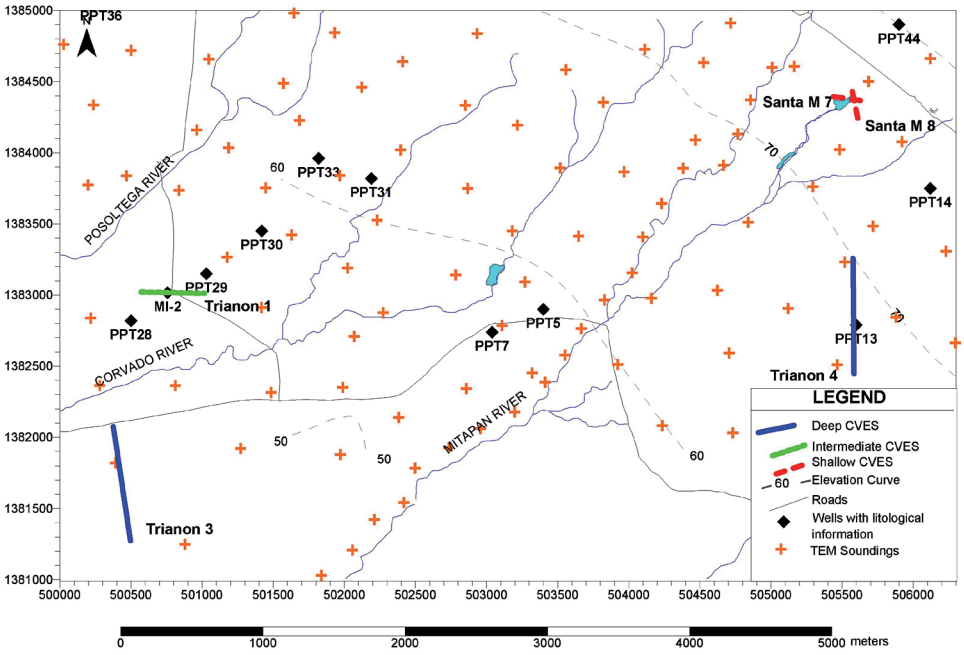


FIGURE 7
Location of the selected CVES together with TEM and boreholes locations with geological information.

to 100 m. However, in the two southern-most of these locations the depth to the conductor is based on only one sounding. At the edges of the contoured maps, certain contour errors are observed as pixels with colours different from the surrounding pixels. The colours of these pixels are not supported by any data points and are clearly contouring errors.

Resistivities around 1 Ωm are very low and usually associated with sulphides, heavy clays or mineral rich groundwater. Sulphides are not expected in this area and have not been found in any of the boreholes. Mineral rich groundwater could potentially be present because of saltwater intrusion or in connection with the hydrothermal activity in the area. However electrical conductivity measurements of the groundwater in boreholes have revealed groundwater resistivities between 9–100 Ωm. Hence, mineral rich groundwater does not explain the low resistivities. Therefore the good conductor is interpreted as a layer of weathered saprolite. Saprolite is highly conductive when formed over mafic rocks such as the Tamarindo Formation due to the formation of clay minerals. This saprolite is interpreted as part of the Las Sierras Formation underlying the quaternary deposits described in the geological framework section.

## CVES profiles

A total of 50 CVES profiles were carried out in the León-Chinandega plains from 1999–2005. Four different electrode configurations were used during this project: Wenner, Schlumberger, pole-dipole and multiple gradient. An approximate length of 45 km was covered with a maximum depth of penetration range in the inverted models from 36–222 m. The depth penetration of the survey depends primarily on the electrode separation and the electrode array configuration and secondarily on the resistivity distribution in the earth.

Five CVES profiles located in the central part of the plains are presented (Fig. 7). They are located in an area between the Posoltega and Quezalguaque rivers in the southern part of the TEM grid.

Most of the boreholes in the area are intended for irrigation purposes and are drilled to depths between 25–65 m, depending on the productivity of the penetrated layers and are located within the pyroclastic and alluvial deposits. One exception is borehole MI-2, with a depth of 147 m. It was drilled for hydrogeological investigation purposes (INETER 2000).

### *Shallow penetration CVES*

CVES Santa Maria 7 and Santa Maria 8 were carried out over the Santa Maria spring. The separation between electrodes was three metres and the Wenner multi-electrode array was used. The maximum depth of the inverted sections was 36 m and the total lengths of the CVES profiles were 240 m and 300 m, respectively, for Santa Maria 7 and Santa Maria 8.

The inverted sections show that the springs (their location are identified in the inverted section as vertical black lines) are formed when the water table reaches the surface (depression springs).

The geological information from boreholes PPT-44 and PPT-14 shows that the materials are mainly composed of silt with subordinate sands and gravels. Below 30 m depth the silty sediments contain more clay (Corriols 2003).

The inverted sections show three well-defined geo-electrical layers. At the top is a high resistivity layer (above 52 Ωm) associated with dry silty material. Underlying this unit is a medium resistivity layer (27–52 Ωm) associated with the recent pyroclastic and alluvial deposits. The bottom layer is a low resistivity layer (below 27 Ωm), probably associated with the presence of

clay enriched materials (see Fig. 8). The high resistance zones in the top layer are associated with consolidated material.

*Medium penetration CVES*

CVES El Trianon-1 is located south of Posoltega River. The inverted sections show two well- defined geo-electrical layers; at the top a medium resistivity layer (10–27 Ωm) associated with dry silty materials and an underlying medium resistivity layer (27–52 Ωm) associated with the volcanic materials. Below this unit a low-resistivity layer is found (below 10 Ωm), probably associated with the presence of clay enriched materials (see Fig. 9). The absence of the top high resistivity layer in this profile is probably due to the shallow water table in the area (around 1 m).

*Deep penetration CVES*

CVES El Trianon-2 and El Trianon-3 are presented as examples of deep penetration CVES. The separation between electrodes was 10 metres and the pole-dipole multi-electrode array was used, including forward and reverse measurements. The maximum depth of the inverted section was 220 m and the total length of the profile was 800 m.

The inverted sections show four distinct geo-electrical layers. The top layer can be associated with the non saturated zone (with resistivities from 7–14 Ωm). The second layer can be associated with the volcanic and alluvial deposits with an interpreted thickness around 40 m and an increase of the resistivity values (up to 37 Ωm). Underlying the second layer is a very low (below 7 Ωm) resistivity unit with a thickness in the inverted model of around 100 m. This layer can be associated with the Las Sierras Formation. At the bottom of the inverted section, high resistivity (more than 140 Ωm) regions can be observed that can be associated with the Tamarindo Formation (see Fig. 10).

## CONCLUSIONS

The TEMfast 48 equipment tests, carried out at Lyngby in Denmark, showed that after calibration the measured response

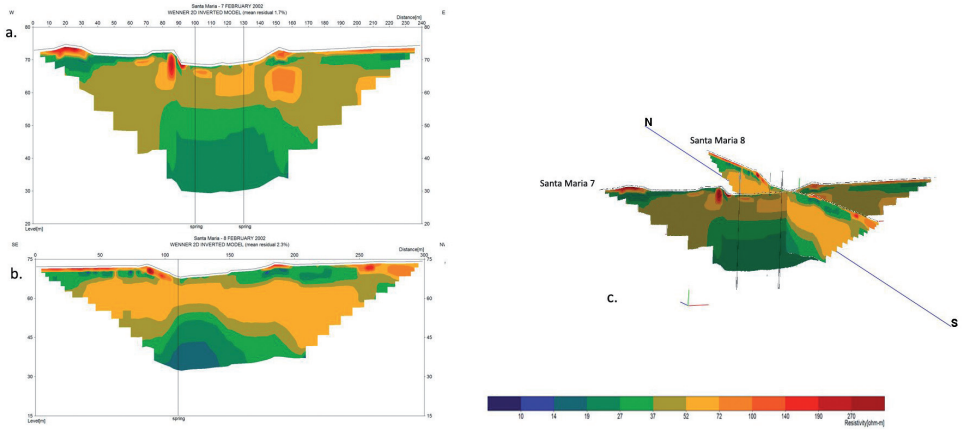


FIGURE 8
a) CVES Santa Maria 7, b). CVES Santa Maria 8, c) fence diagram showing the relation between the Santa Maria CVES sections.

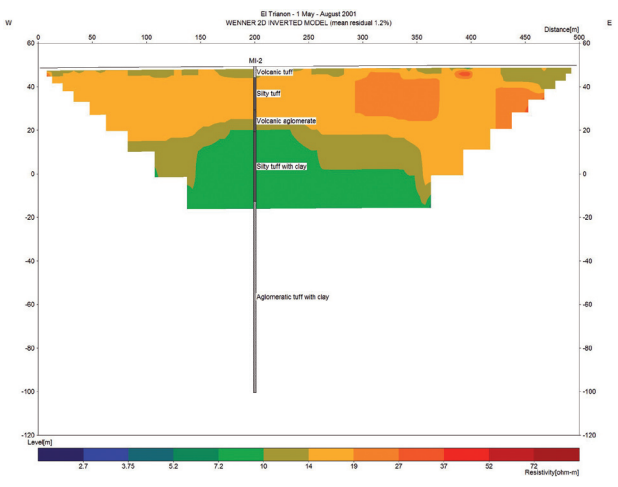


FIGURE 9
Inverted section for CVES El Trianon-1, with borehole MI-2.

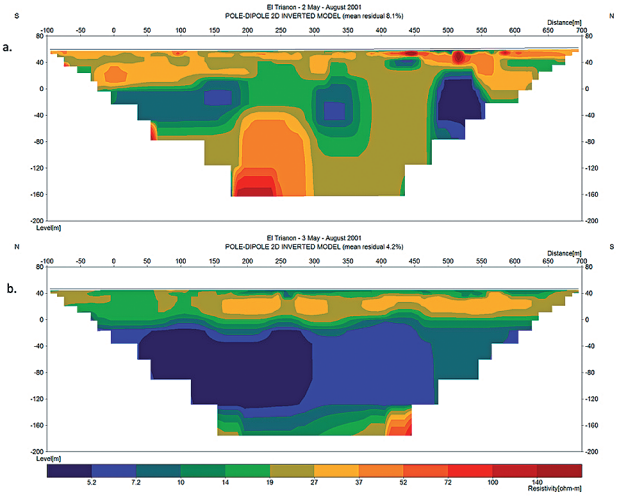


FIGURE 10
Deep CVES profiles.

gave a model corresponding to the test site model. A coincident 25 m × 25 m loop was found to be optimal. The TEM equipment worked very well in the field and is optimal in areas difficult to access, due to its compactness and lightness.

At large-scale the TEM investigation revealed a regular three-layered geoelectrical model with simple structures over the majority of the area except for the coastal regions. The survey area is characterized by volcanic deposits and alluvial sediments of volcanic origin and the top layer is composed of dry young volcanic materials. The boundary of the underlying layer defines the groundwater surface. In some areas the groundwater surface is very shallow and the thin soil cover is not resolved. The third layer is a conductive clay rich formation interpreted to be a weathered saprolite layer covering the Tamarindo basement. In the coastal regions, the geology is complex due to outcrops of the Tamarindo Formation.

The 1D inversion results appeared to be robust and reliable and the TEM method turned out to be applicable in the survey area. The general geophysical model of the TEM survey corresponds with the results of the CVES investigation. At smaller scale the CVES investigation revealed more complex conditions locally, which were not resolved by the TEM investigation. This is partly because of less dense TEM data density locally and partly because of the resolution differences of the two methods.

Resistivities below 1 Ωm with CVES are only found in the coastal region (due to the presence of marine intrusion), whereas TEM suggests resistivities below 1 Ωm in the Posoltega-Quezalguaque area as well as in the coastal region. As the strength of the TEM method is to resolve low resistivities, the low resistivities found in other parts of the investigated area by the TEM investigation are likely to be correct. The differences in the results may be attributed to equivalence effects.

The CVES results show two well defined hydrogeophysical units that can be associated with the hydrostratigraphy defined in the geological framework section. The upper hydrogeophysical unit is identified as the principal aquifer. With medium resistivity values and thickness around 60 m, this unit extends along the plain and lenses of different materials can be found. From the geological information, this section can be associated with the pyroclastic and alluvial deposits. The lower hydrogeophysical unit is characterized by lower resistivity values with thickness from 100 m, which in the deeper parts can reach up to 250 m and it can be associated with the Las Sierras Formation. Some of the deep CVES profiles show areas of high resistivity below the second hydrogeophysical unit and it is interpreted as the Tamarindo Formation.

The geophysical data collected in the present study is an important step for the understanding of the groundwater systems within the study area. The National Autonomous University of Nicaragua and Lund University are working together in hydrogeological investigations to increase the understanding of the contribution of groundwater residence times and biodegradation to persistence and effects of pesticides in groundwater.

**ACKNOWLEDGEMENTS**

This investigation was performed with economic support from the Swedish International Development Authority (Sida-SAREC), as part of a multi-disciplinary cooperation programme between Lund University and the Autonomous University of Nicaragua (UNAN-Managua). We want to thank the Department of Earth Sciences, Aarhus University, Denmark and INETER (Nicaraguan Institute of Territorial Researches) for supporting part of the field work investigation in this area and Sugar States Limited (Ingenio San Antonio) for their help and permission during the different stages of the geophysical surveys. Thanks to Tom Hagensen for his voluntary participation in the fieldwork in Nicaragua. We also want to thank Gustaf Lind at the Earth Sciences Centre, Gothenburg University, for generously lending us their TEMfast48 instrument.

**REFERENCES**

AEMR. 2002. *TEM-RESEARCHER, Version 6, Manual Applied Electromagnetic Research* AEMR.

Auken E., Jørgensen F. and Sørensen K.I. 2003. Large-scale TEM investigation for groundwater. *Exploration Geophysics* **33**, 188–194.

Becker A. and Cheng G. 1988. Detection of repetitive electromagnetic signals. In: *Electromagnetic Methods in Applied Geophysics* (ed. M.N. Nabighian), pp. 365–441. SEG.

Briemberg J. 1994. *An Investigation of Pesticide Contamination of Groundwater Sources for Urban Water Distribution Systems in the Pacific Region of Nicaragua*. Proctor and Redfern International Ltd. Instituto Nicaragüense de Acueductos y Alcantarillados, INAA. Managua, Nicaragua.

Cáceres V. 2005. *Caracterización de las Propiedades Resistivas de los Acuíferos Someros en la Zona Central de la Planicie de León-Chinandega* (Characterization of the Resistivity Properties of Shallow Aquifers in the Central Part of the León-Chinandega Plain). PhD thesis, Facultad de Ciencias e Ingenierías. Universidad Nacional Autónoma de Nicaragua, Nicaragua.

Calderón H. 2003. *Numerical modeling of the groundwater flow system in a sub-basin of the León-Chinandega aquifer, Nicaragua*. MSc thesis, Department of Geology and Geophysics, University of Calgary.

Calderon Palma H. and Bentley L.R. 2007. A regional-scale groundwater flow model for the Leon-Chinandega aquifer, Nicaragua. *Hydrogeology Journal* **15**, 1457–1472. doi:10.1007/s10040-007-0197-6

Christensen N.B. 1990. Optimized fast Hankel transform filters. *Geophysical Prospecting* **38**, 545–568.

Christiansen A.V. and Christensen N.B. 2003. A quantitative appraisal of airborne and ground-based transient electromagnetic (TEM) measurements in Denmark. *Geophysics* **68**, 523–534.

CIGEO 1999. *Estudio Geofísico de Resistividad Eléctrica entre las subcuencas de los ríos Chiquito y El Realejo, NW de Nicaragua. Volumen I* (Geophysical Survey by Electrical Resistivity Methods within the Sub-basins of Rio Chiquito and El Realejo, NW Nicaragua. Volume 1). Centro de Investigaciones Geocientíficas, CIGEO, UNAN-Managua. Managua, Nicaragua.

Corriols M. 2003. *Hydrogeological, geophysical and hydrochemical investigations in the León-Chinandega plains, Nicaragua.* Licentiate thesis, Lund University.

Corriols M. and Dahlin T. 2008. Geophysical characterization of the León-Chinandega Aquifer, Nicaragua. *Hydrogeology Journal* **16**, 349–362.

Dahlberg C. and Odebjer W. 2002. *Investigation of hydrochemical and pesticide concentrations in groundwater at Posoltega, León-*

*Chinandega plains, Nicaragua. A minor field study*. MSc thesis, Lund University.
Dahlin T. 2001. The development of DC resistivity imaging techniques. *Computers & Geosciences* **27**, 1019–1029.
Delgado V.Q. 2003. *Groundwater flow system and water quality in a coastal plain aquifer in northwestern Nicaragua*. MSc thesis. Department of Geology and Geophysics, University of Calgary.
Effersø F., Auken E. and Sørensen K.I. 1999. Inversion of band-limited TEM responses. *Geophysical Prospection* **47**, 551–564.
Elming S.-Å., Layer P. and Ubieta K. 2001. A paleomagnetic study and age determinations of Tertiary rocks in Nicaragua, Central America. *Geophysical Journal International* **147**, 294–309.
Goldman M. and Kafri U. 2006. Hydrogeophysical applications in coastal aquifers. In: *Applied Hydrogeophysics* (eds H. Vereecken, A. Binley, G. Cassiani, A. Revil and K. Titov), pp. 233–254. Springer.
Hydrogeophysics Group. 2002. Vejledning i kalibrering af TEM måleudstyr. Hydrogeophysics Group, Department of Earth Sciences, University of Aarhus. http://www.hgg.geo.au.dk/rapporter/vejledning_kalibreringssondering_2002.pdf
INETER (Nicaraguan Institute of Territorial Studies). 2000. *Estudios hidrológicos e hidrogeológicos en la región del pacífico de Nicaragua. Fase I, región Chinandega-León-Nagarote. Informe Final* (Hydrologic and hydrogeologic studies in the pacific region of Nicaragua. Phase 1, Chinandega-León-Nagarote region. Final report). Instituto Nacional de Estudios Territoriales, INETER Managua, Nicaragua.
Kuang J. 1971. *Geología de la Costa del Pacífico de Nicaragua. Informe # 3* (Geology of the Pacific Coast of Nicaragua. Report #3). Managua, Nicaragua.
Loke M.H. 2001. *Tutorial: 2-D and 3-D Electrical Imaging Surveys*. http://www.geoelectrical.com.
Loke M.H., Acworth I. and Dahlin T. 2003. A comparison of smooth and blocky inversion methods in 2-D electrical imaging surveys. *Exploration Geophysics* **34**, 182–187.
Lopez A., Lacayo M., Cuadra J. and Picado F. 2000. *Estudio de la Contaminación por Plaguicidas en el Acuifero y Suelos de la Región León-Chinandega, Nicaragua* (Study of Pesticides pollution in the aquifer and soils of the León-Chinandega región, Nicaragua). Centro para la Investigación en Recursos Acuáticos de Nicaragua, CIRA-UNAN, Managua.
McBirney A. and Williams N.S. 1965. *Volcanic History of Nicaragua*. University of California Press.
MenkeW. 1989. *Geophysical Data Analysis: Discrete Inverse Theory*. Academic Press.
Moncrieff J.E., Bentley L.R. and Calderon Palma H. 2008. Investigating pesticide transport in the Leon-Chinandegea aquifer, Nicaragua. *Hydrogeology Journal* **16**, 183–197. doi:10.1007/s10040-007-0229-2
Oldenburg D.W. and Li Y. 1994. Inversion of induced polarisation data. *Geophysics* **59**, 1327–1341.
Ryom M. 2004. *TEMfast 48 test and investigations in Nicaragua*. MSc thesis, Department of Earth Sciences, University of Aarhus.
Tsourlos P. 1995. *Modeling interpretation and inversion of multielectrode resistivity survey data*. PhD thesis, Department of Electronics, University of York.
United Nations. 1974. *Investigaciones de Aguas Subterráneas en la Región del Pacífico de Nicaragua. Volumen I. Zona de Chinandega* (Groundwater Investigations in the Pacific Region of Nicaragua. Volume 1. Chinandega Zone). Nueva York, USA.
Wilson T.C. 1942. *Summary Report Geology of the Pacific Coast Area, Nicaragua*. Managua, Nicaragua.
Zoppis-Bracci L. and Del Guidicce D. 1958. *Geologia de La Costa del Pacifico de Nicaragua* (Geology of the Pacific Coast of Nicaragua). Boletin del servicio Geologico Nacional, Managua, Nicaragua.

## APPENDIX – TEMFAST 48 EQUIPMENT, DESCRIPTION AND TESTS

### Introduction

The TEMfast 48 system differs from other TEM systems by being very compact and lightweight, which makes the equipment very attractive. However, the available information about the system details was inadequate to perform reliable inversions (Effersø *et al.* 1999). Therefore, the TEMfast 48 system was tested at the Lyngby TEM-test site outside Aarhus in Denmark prior to the field campaign in Nicaragua. This test site was established in 2001 with the purpose of testing and calibrating TEM equipment (Hydrogeophysics Group 2002). The tests include a comparison of TEMfast 48 measurements with several different settings and configurations with the standard model response at the test site. Communicating and disseminating these results is of great importance for the future use of the system.

### Description

The TEMfast 48 system has been developed by the Russian Applied Electromagnetic Research Company (AEMR LTD.). The complete TEMfast 48 set, including cables, battery and PC, fits into a small backpack and weighs approximately 5 kg. The TEMfast 48 device itself includes transmitter, receiver, controller and battery assembled in a single case. The system is operated by the TEMfast 48 HPC software that runs on a hand-held computer.

The internal 12 V, 2000 mAh battery can supply power for approximately 50 soundings. Depending on the battery and resistance of the loop cable, either 1 A or 4 A can be transmitted (AEMR 2002).

Aside from the physical properties of the instrument, the TEMfast 48 system also differs from other TEM systems in other ways. The transmitter does not apply a 1/1 pulse/pause ratio with alternating polarity as most systems. Instead the TEMfast 48 uses a sequence of uni-polar rectangular current pulses with a pulse/pause ratio of 3/1 (AEMR, 2002). The result of the on-time being longer than the pause off-time is that the turn-on effects will be minimal when the current is turned off and the measurements are started. Without the turn-on effects it is possible to immediately transform the responses to apparent resistivity and perform assessments of the data in the field. However, the consequence of a longer on-time will be fewer stacks of the signal in a given measuring time period compared to equipment with 1/1 pulse/pause ratio. Additionally, the turn-on ramp is modelled in most interpretation software to get rid of turn-on effects and therefore the longer on-time is less important for the final result. TEMfast 48 transmits uni-polar current that differs from the alternating polarity that is often applied to avoid influence of low-frequency noise and instrumental drift (Becker and Cheng 1988). How these problems are overcome in TEMfast 48 is not described but supposedly a random gridding is applied meaning that the pulse/pause ratio is not exactly 3/1 but is randomly chosen close to 3/1.

The TEMfast 48 receiver integrates the analog signal over time gates with lengths increasing exponentially with time. The first gate-centre time is approximately 4 μs after the current is turned off (AEMR 2002), which initiates measurements earlier than other systems. By measuring these early times it should be theoretically possible to gain information about shallow layers. However, it is uncertain whether the equipment is ready for registering reliable measurements this early, which will depend on the applied loop-size and transmitted current.

**Equipment tests**

Different configurations were tested at the Lyngby TEM-test site. The tests showed that a 25 m x 25 m coincident loop configuration was the optimal setup. Central loop configurations were disturbed at early times. Smaller loops (15 m × 15 m and 20 m × 20 m) had a poorer signal-to-noise ratio at late times and a larger loop (40 m × 40 m) had the first two data points disturbed. Transmitting 1 A gave a smooth signal curve at early times whereas the first three data points were useless when transmitting 4 A.

The maximum off-time is chosen between 9 possible time-key settings. The longer the off-time, the less the signal is analog stacked. This was clearly seen by the fact that soundings with long recording times were noisier at late times. A maximum recording time of 2 ms was found to be optimal under the conditions at the test site. However, in areas with lower noise, longer recording times can be applied.

The digital stack-setting is a choice between the numbers 1–20. All digital stack-settings were tested and no significant difference was observed. However, there is a considerable difference in the duration of a measurement depending on the stack setting. A choice of a digital stack setting of 10 seemed a reasonable choice.

Oscilloscope measurements were performed in order to obtain information about the actual turn-off time, pulse/pause-ratio and total on-off-time period to be used in the inversion. The following results were obtained and applied in the inversion:

Finally, a sounding with the optimal TEMfast 48 configuration was compared to the standard model response at the test site. The standard model is the calculated forward response of the known earth model at the test site with the actual configuration. Since the internal filters of the TEMfast 48 equipment are not known, the forward response is calculated with several different filters in order to compare these with the actual measurements at the site. This comparison will help to decide which filter to include in the inversion. Finally, the comparison will reveal which calibration parameters should be applied in the inversion. Calibration by shifting the data amplitude by a certain factor compensates for errors in the determination of the transmitted current. Calibration by shifting the delay time by a certain constant compensates for variation in turn-off, waveform, synchronization between receiver and transmitter and in this case the missing information about precise filter characteristics.

The correlation between the forward responses and the calibrated TEMfast 48 coincident test site measurement (Fig. 11) shows that the calibrated sounding corresponds to a forward modelled response with a 250 KHz filter. The TEMfast 48 sounding is calibrated with an amplitude factor of 1.14 and a time constant of 0.5 $\mu$s. These calibration parameters are used in the inversion of all the TEMfast 48 data collected in Nicaragua.

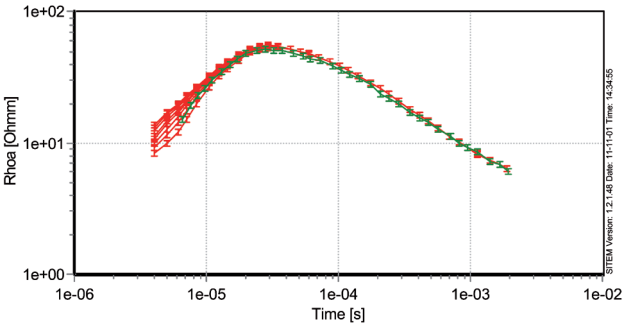


FIGURE 11

The green response curve is the calibrated TEMfast 48 sounding on the test site. The red curves are the forward responses of the test site model with corresponding setup but with different filters included in the calculation. From lowest red curve upwards are the modelled responses with 200 KHz, 250 KHz, 300 KHz, 350 KHz, 400 KHZ, 500 KHz, 600 KHz and 700 KHz filters respectively.

| Loop size | Maximum recording time | Transmitted current | Turn-off time | Pulse/pause ratio | Total on-off-time period | Repetition frequency |
|---|---|---|---|---|---|---|
| 25 m × 25 m | 2 ms | 1 A | 3.0 $\mu$s | 3/1 | 10 ms | 100 Hz |
| 25 m × 25 m | 4 ms | 1 A | 3.3 $\mu$s | 1/1 | 30 ms | 33.33 Hz |
| 25 m × 25 m | 8 ms | 1 A | 2.9 $\mu$s | 3/2 | 50 ms | 20 Hz |
| 25 m × 25 m | 2 ms | 2.2 A | 3.3 $\mu$s | 3/1 | 10 ms | 100 Hz |
| 25 m × 25 m | 4 ms | 2.2 A | 3.3 $\mu$s | 1/1 | 30 ms | 33.33 Hz |
| 25 m × 25 m | 8 ms | 2.2 A | 3.0 $\mu$s | 3/2 | 50 ms | 20 Hz |